Stability Margin Improvement of Vehicular Platoon Considering Undirected Topology and Asymmetric Control

Yang Zheng, Shengbo Eben Li, *Member, IEEE*, Keqiang Li, and Le-Yi Wang, *Fellow, IEEE*

***Abstract*— The platooning of autonomous vehicles has the potential to significantly improve traffic capacity, enhance highway safety, and reduce fuel consumption. This paper studies the scalability limitations of large-scale vehicular platoons moving in rigid formation, and proposes two basic ways to improve stability margins, i.e., enlarging information topology and employing asymmetric control. A vehicular platoon is considered as a combination of four components: 1) node dynamics; 2) decentralized controller; 3) information flow topology; and 4) formation geometry. Tools, such as the algebraic graph theory and matrix factorization technique, are employed to model and analyze scalability limitations. The major findings include: 1) under linear identical decentralized controllers, the stability thresholds of control gains are explicitly established for platoons under undirected topologies. It is proved that the stability margins decay to zero as the platoon size increases unless there is a large number of following vehicles pinned to the leader and 2) the stability margins of vehicular platoons under bidirectional topologies using asymmetric controllers are always bounded away from zero and independent of the platoon size. Simulations with a platoon of passenger cars are used to demonstrate the findings.**

***Index Terms*— Autonomous vehicles, decentralized control, platoon, scalability, stability margin.**

I. Introduction

DURING the past few decades, the increasing traffic demand brings a heavy burden on the existing transportation infrastructure and sometimes leads to a heavily congested road network [1]. The platooning of autonomous vehicles has the potential to improve traffic capacity and smoothness, enhance highway safety, and reduce fuel consumption [2], which has recently received extensive research interests (see [2]–[6], and the references therein). The main objective of vehicular platoon control is to ensure that all the vehicles maintain the desired speed and keep a prespecified formation geometry that is dictated by the intervehicle spacing policy.

To the best of our knowledge, the earliest practices on platoon control date back to the PATH program during the late 1980s in California [4]. Since then, many topics have been discussed for platoon control, such as selection of spacing policies [5], [6], the influence of information flow topologies [7]–[10], powertrain dynamics and communication delay [11], [12], and homogeneity and heterogeneity [13]. In addition, many advanced control methods have been introduced into platoon automation to achieve better performances. For instance, Liang and Peng [14] proposed an optimal control strategy for the upper-level controller to guarantee string stability. Stankovic *et al.* [15] used the inclusion principle to decompose an interconnected vehicular platoon into locally decoupled subsystems, for which decentralized overlapping controllers were designed. Dunbar and Caveney [16] proposed a distributed receding horizon controller for vehicular platoon, and derived the sufficient conditions to ensure asymptotic stability. More recently, some demos of vehicular platoon have been performed in the real world, including the GCDC in the Netherlands [17], SARTRE in Europe [18], and Energy-ITS in Japan [19]. A recent review on platoon control can be found in [20].

One recent research focus of platooning is on finding the essential performance limitation of large-scale platoons, e.g., the bound of error amplification, trend of stability deterioration, and scalability with increasing platoon size [21]–[29]. Seiler *et al.* [21] showed that due to a complementary sensitivity integral constraint, there was a scalability limitation for platoon with linear identical controllers under predecessor-following topology. Barooah and Hespanha [22] further pointed out that for a homogeneous platoon under bidirectional (BD) topology, linear identical controllers also suffered fundamental limitation on the closed-loop stability due to amplified spacing errors and disturbances. Middleton and Braslavsky [23] extended the work in [21] by considering heterogeneous vehicle dynamics, limited communication range, and nonzero time headway policy within the platoon formulation, and showed that both forward communication range and small time headway cannot alter the string instability. Even for general undirected information flow (UIF) topology, under which vehicles can obtain information beyond

Manuscript received November 05, 2014; revised June 16, 2015; accepted September 20, 2015. Date of publication October 16, 2015; date of current version June 9, 2016. This work was supported in part by the Chinese National Programs for High Technology Research and Development through the Ministry of Science and Technology, China, under Grant 2012AA111901 and in part by the National Natural Science Foundation of China under Grant 51205228 and Grant 51575293. Recommended by Associate Editor C. Canudas-de-Wit. *(Yang Zheng and Shengbo Eben Li equally contributed to this work.) (Corresponding author: Shengbo Eben Li.)*

Y. Zheng and K. Li are with the State Key Laboratory of Automotive Safety and Energy, Tsinghua University, Beijing 100084, China (e-mail: zhengy13@mails.tsinghua.edu.cn; likq@tsinghua.edu.cn).

S. E. Li is with the State Key Laboratory of Automotive Safety and Energy, Department of Automotive Engineering, Tsinghua University, Beijing 100084, China (e-mail: lisb04@gmail.com).

L.-Y. Wang is with the Department of Electrical and Computer Engineering, Wayne State University, Detroit, MI 48202 USA (e-mail: lywang@wayne.edu).

Color versions of one or more of the figures in this paper are available online at http://ieeexplore.ieee.org.

Digital Object Identifier 10.1109/TCST.2015.2483564

their nearest neighbors, Darbha and Pagilla [24] pointed out the limitation of identical controllers to maintain a rigid formation and indicated that there was a critical platoon size beyond which the motion would lose stability.

The following two major approaches have been proposed to analyze the above-mentioned performance limitations and improve the scalability of large-scale platoons.

1) The matrix theory-based approach that directly analyzes the limit of stability and performance in the time domain.
2) The partial differential equation (PDE) approximation-based approach that approximates the platoon dynamics into a continuous PDE and then studies the eigenvalues of the corresponding PDE.

Using the first approach, Lin *et al.* [27] investigated the scalability of a large-scale vehicular platoon with an optimal controller design and showed that nonsymmetric controllers can yield better scaling trends and enhance formation coherence. For high-dimensional formations, Bamieh *et al.* [25] demonstrated that localized symmetric feedback can also regulate large-scale disturbances. In [29], it was shown that the asymmetric control gains can make the control architecture highly scalable, since the stability margin of the closed loop can always be bounded away from zero. Using the second approach, i.e., the PDE approximation, Barooah *et al.* [26] showed that the closed-loop stability margin could be significantly improved by introducing small amounts of mistuning to symmetric control gain. Adopting similar strategies to [26], Hao *et al.* [28] proved that the scaling law for the stability margin could be significantly improved by employing a higher dimensional information flow topology or by introducing small asymmetry in the control gain. In summary, both approaches are able to analyze the scalability of the vehicular platoon. However, for the first approach, most research relies on the assumption of idealized double-integrator models for vehicle dynamics. The assumption of double integrators simplifies the mathematical analysis, but does not capture many practical characteristics, e.g., inertial lags in powertrain dynamics, which should not be neglected in real-world implementation [11], [14], [15], [17]. For the second approach, the PDE approximating technique can avoid the difficulties of analyzing high-dimensional matrices and gain insights into the effect of local controllers on the scalability, but it inevitably introduces approximation errors and is suitable only for vanishingly small asymmetric structures because of using perturbation theory. In addition, the PDE technique is applicable only to limited kinds of information topologies, like BD topology [26], [28].

In this paper, we directly take inertial lags of powertrain dynamics into consideration for the stability margin analysis of large-scale platoons. This consideration provides more accurate prediction of the scalability limitation in real-world implementation. Moreover, the stability margin analysis is conducted based on the high-dimensional matrix factorization instead of the PDE approximation. The benefit is that we can not only model more general undirected topologies, but also extend the analysis to the case of a large asymmetric control. By employing tools, such as algebra graph theory, matrix factorization, and eigenvalue analysis, the analysis further shows how to improve the stability margin of a homogeneous platoon in terms of topology selection and control adjustment from a unified viewpoint. The main contributions of this paper are as follows.

1) A closed-loop stability theorem for homogeneous platoons interconnected by the UIF topology is derived using the Routh–Hurwitz stability criterion and Rayleigh–Ritz theorem. This theorem explicitly establishes the stabilizing thresholds of linear control gains and characterizes the scalability limitation for platoons under the UIF topology. Moreover, it is shown that extending information flow to reduce the tree depth is one major way to recover the loss of stability margins and achieve a scalable platoon. The results in this theorem are extensions of [9] and [24], in which inertial lags of vehicle powertrains were neglected and each vehicle was modeled as a point mass.
2) Under an asymmetric control structure, the scalability of platoons under the BD topology is established, which indicates that employing asymmetric control is another way to improve stability margins of large-scale platoons. The proof is based on the matrix factorization technique and eigenvalue analysis, showing that the stability margin of such a platoon is bounded away from zero and independent of the platoon size. This finding conforms to the results in [26] and [28], which adopted the PDE approximation and was suitable only for vanishingly small asymmetric structures. The matrix-based approach is used in this paper, and as such, the results are more accurate and can be extended to larger asymmetric degrees. In addition, our finding greatly extends the main results in [29], in which the double-integrator model is used, which makes stability analysis straightforward, but departs from the reality of powertrain dynamics.

The remainder of this paper is organized as follows. Section II introduces the problem formulation of platoon control. Section III presents two theorems for homogeneous platoon: 1) the closed-loop stability and scalability theorem for the UIF topology with identical controllers and 2) the scalability theorem for the BD topology with asymmetric controllers. Numerical simulations are shown in Section IV. Finally, Section V presents the conclusion.

II. Problem Formulation

This paper considers a platoon on a flat road (see Fig. 1), which aims to move at the same speed while maintaining a rigid formation geometry. The platoon has $N+1$ vehicles (or nodes), including a leading vehicle indexed by 0 and N following vehicles indexed from 1 to N.

As demonstrated in Fig. 1, a platoon consists of four main components: 1) vehicle dynamics; 2) decentralized controller; 3) information flow topology; and 4) formation geometry. The vehicle dynamics describe the behavior of each node; the information flow topology defines how nodes exchange information with each other; the decentralized controller implements feedback control for each vehicle; and the formation geometry dictates the desired distance between any two successive nodes.

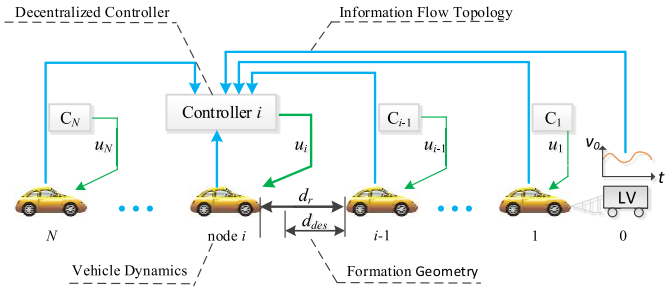

Fig. 1. Four major components of a platoon. 1) Vehicle dynamics. 2) Information flow topology. 3) Decentralized controller. 4) Formation geometry. d_r is the actual relative distance, d_{des} is the desired distance, u_i is the control signal for the ith vehicle, and C denotes the controller.

Notations: The real and complex domains are denoted by $\mathbb{R}$ and $\mathbb{C}$, respectively. The real part of a complex number $s \in \mathbb{C}$ is denoted by $\text{Re}(s)$, and the imaginary part by $\text{Im}(s)$. The set of $m \times n$ real matrices is denoted by $\mathbb{R}^{m\times n}$. The transpose of a vector or a matrix A is denoted by A^T. We define $\mathbf{1_n} = [1, 1, \ldots, 1]^T \in \mathbb{R}^{n\times 1}$, and use I_n as the identity matrix of dimension n. Let $\sigma_i(A)$ denote the ith eigenvalue of matrix $A \in \mathbb{R}^{n\times n}$, $i = 1, 2, \ldots, n$, and all its eigenvalues are represented in an increasing order of their real parts, i.e., $\text{Re}(\sigma_{\min}(A)) \le \text{Re}(\sigma_2(A)) \le \cdots \le \text{Re}(\sigma_{n-1}(A)) \le \text{Re}(\sigma_{\max}(A))$. The spectrum of A is denoted by $S(A) = \{\sigma_{\min}(A), \ldots, \sigma_{\max}(A)\}$. $\text{diag}\{a_1, a_2, \ldots, a_n\}$ denotes a diagonal matrix whose diagonal entries starting at the upper left corner are $a_1, a_2, \ldots, a_n$. Let $A \in \mathbb{R}^{m\times n}$ and $B \in \mathbb{R}^{p\times q}$, then $A \otimes B$ is the Kronecker product of A and B

$$A \otimes B = \begin{bmatrix} a_{11}B & \cdots & a_{1n}B \\ \vdots & \ddots & \vdots \\ a_{m1}B & \cdots & a_{mn}B \end{bmatrix} \in \mathbb{R}^{mp\times nq}.$$

A. Model for Node Dynamics

The platoon is assumed to be homogeneous, as studied in [7]–[9], [21], and [22]. The longitudinal dynamics of each node are composed of engine, drive line, brake system, aerodynamics drag, tire friction, rolling resistance, and gravitational force. The following assumptions are used [5], [11], [30], [31].

1) The powertrain dynamics are lumped into a first-order inertial transfer function.
2) The vehicle body is considered to be rigid and symmetric.
3) The influence of pitch and yaw motions is neglected.
4) The driving and braking torques are integrated into one control input.

Then, the model of vehicle longitudinal dynamics becomes

$$\begin{cases} \dot{s}_i(t) = v_i(t) \\ \dot{v}_i(t) = \dfrac{1}{M}\left(\eta_T \dfrac{T_i(t)}{R_w} - C_A v_i^2 - Mgf\right), \quad i = 1, 2, \ldots, N \\ \tau \dot{T}_i(t) + T_i(t) = T_{i,\text{des}}(t) \end{cases} \tag{1}$$

where $s_i(t)$ and $v_i(t)$ denote the position and velocity of node i, respectively, M is the vehicle mass, C_A is the coefficient of aerodynamic drag, g is the gravity constant, f is the coefficient of rolling resistance, $T_i(t)$ is the actual driving/braking torque, $T_{i,\text{des}}(t)$ denotes the desired driving/braking torque, τ is the inertial lag of vehicle longitudinal dynamics, R_w is the tire radius, and η_T is the mechanical efficiency of the driveline. The position, velocity, and acceleration of the leader are denoted by $s_0(t)$, $v_0(t)$, and $a_0(t)$, respectively. The leader tracks a constant speed reference trajectory, i.e., $a_0(t) = 0$, $s_0 = v_0 t$.

The exact feedback linearization technique is used to convert the nonlinear model (1) into a linear one. The same technique has been widely used in platoon control (see [7], [11], [15]). The output of position with relative degree three is used to construct the feedback linearization law, as shown in the following:

$$T_{i,\text{des}}(t) = \frac{1}{\eta_T}\left(C_A v_i\left(2\tau \dot{v}_i + v_i\right) + Mgf + Mu_i\right) R_w \tag{2}$$

where u_i is the control input after linearization. Then, we have

$$\tau \dot{a}_i(t) + a_i(t) = u_i(t) \tag{3}$$

where $a_i(t) = \dot{v}_i(t)$ denotes the acceleration of node i. For the sake of platoon control, a third-order state-space model is derived for node i

$$\begin{aligned} \dot{x}_i(t) &= Ax_i(t) + Bu_i(t) \\ A &= \begin{bmatrix} 0 & 1 & 0 \\ 0 & 0 & 1 \\ 0 & 0 & -\dfrac{1}{\tau} \end{bmatrix}, \quad B = \begin{bmatrix} 0 \\ 0 \\ \dfrac{1}{\tau} \end{bmatrix} \end{aligned} \tag{4}$$

where $x_i(t) = [s_i, v_i, a_i]^T$ is the state of node i, and $u_i(t)$ is the control input of node i after linearization.

B. Model for Information Flow Topology

The information flow among the platoon is modeled by a directed graph $G = \{V, E\}$, in which $V = \{0, 1, 2, \ldots, N\}$ is the set of nodes and $E \subseteq V \times V$ is the set of edges in connection. The following three matrices are used to represent the properties of information flow modeled by G: 1) adjacent matrix $\mathcal{A}$; 2) Laplacian matrix $\mathcal{L}$; and 3) pinning matrix $\mathcal{P}$. This technique is known as the algebraic graph theory [32], which has been widely used in the area of multiagent control or networked control [8], [32], [33].

The adjacent matrix associated with graph G is defined as $\mathcal{A} = [a_{ij}] \in \mathbb{R}^{N\times N}$ with each entry defined as

$$\begin{cases} a_{ij} = 1, & \text{if } \{j, i\} \in E \\ a_{ij} = 0, & \text{if } \{j, i\} \notin E, \end{cases} \quad i, j = 1, \ldots, N \tag{5}$$

where $\{j, i\} \in E$ means there is a directional edge from node j to node i, i.e., vehicle i receives the information of vehicle j by either wireless communication or radar-based detection. It is assumed that there are no self-loops, i.e., $a_{ii} = 0$, $i = 1, \ldots, N$. Node j is said to be a neighbor of node i if $a_{ij} = 1$, and the neighbor set of node i is denoted by

$$\mathbb{N}_i = \{j | a_{ij} = 1\}.$$

The Laplacian matrix $\mathcal{L} = [l_{ij}] \in \mathbb{R}^{N\times N}$ associated with graph G is defined as

$$l_{ij} = \begin{cases} -a_{ij}, & i \neq j \\ \sum_{k=1}^{N} a_{ik}, & i = j, \end{cases} \quad i, j = 1, \ldots, N. \tag{6}$$

The pinning matrix $\mathcal{P}$ represents how each follower connects to the leader, defined as

$$\mathcal{P} = \text{diag}\{p_1, p_2, \ldots, p_N\} \tag{7}$$

where $p_i = 1$ if edge $\{0, i\} \in E$; $p_i = 0$ otherwise. If $p_i = 1$, vehicle i is said to be pinned to the leader. We define leader accessible set of node i as

$$\mathbb{P}_i = \begin{cases} \{0\}, & \text{if } p_i = 1 \\ \emptyset, & \text{if } p_i = 0. \end{cases}$$

It is assumed that the graph G contains at least one spanning tree rooting from the leader for the controllability of system [33]. A spanning tree is a tree formed by graph edges that connect all the nodes of the graph. In other words, the leader is globally reachable and every follower can obtain the leader information directly or indirectly.

C. Design of Decentralized Controllers

The objective of platoon control is to track the speed of the leader while maintaining a rigid formation governed by the constant distance policy

$$\begin{cases} \lim_{t\to\infty} \|v_i(t) - v_0(t)\| = 0 \\ \lim_{t\to\infty} \|s_{i-1}(t) - s_i(t) - d_{i-1,i}\| = 0, \end{cases} \quad i = 1, 2, \ldots, N \tag{8}$$

where $d_{i-1,i}$ is the desired space between nodes $i-1$ and i. The selection of $d_{i-1,i}$ determines the geometry formation of the vehicular platoon. Here, the constant spacing policy is used for the benefit of high traffic throughput, which has been widely used before (see [7], [9], [16], [21], [22], [24]–[29]).

The local controller of node i only uses its neighborhood information specified by $\mathbb{I}_i = \mathbb{N}_i \cup \mathbb{P}_i$. This local controller is linear

$$u_i(t) = -\sum_{j\in\mathbb{I}_i} [k_{ij,s}(s_i - s_j - d_{i,j}) + k_{ij,v}(v_i - v_j) + k_{ij,a}(a_i - a_j)] \tag{9}$$

where $k_{ij,\#}$ $(\# = s, v, a)$ is the controller gain. A control law satisfying (9) is said to have structure G, whereas an unstructured control law is one that corresponds to a complete graph that requires communications between any pair of vehicles. It should be noted that we are interested in static and linear control laws governed by G. Thus, a communication link, if it exists, is assumed to be perfect in the sense that we ignore the effects such as quantization issues, data dropouts, and data delay.

To rewrite (9) into a compact form, we define the new tracking error $\tilde{x}_i(t)$ for node i

$$\tilde{x}_i(t) = x_i(t) - x_0(t) - \tilde{d}_i \tag{10}$$

where $\tilde{d}_i = [d_{i,0}, 0, 0]^T$. Then, (9) is rewritten into

$$u_i(t) = -\sum_{j\in\mathbb{I}_i} k_{ij}^T(\tilde{x}_i - \tilde{x}_j) \tag{11}$$

where $k_{ij} = [k_{ij,s}, k_{ij,v}, k_{ij,a}]^T \in \mathbb{R}^{3\times 1}$ is the vector of control gains for node i.

D. Formation of Closed-Loop Platoon Dynamics

To derive the platoon dynamics, we define $X = [\tilde{x}_1^T, \tilde{x}_2^T, \ldots, \tilde{x}_N^T]^T \in \mathbb{R}^{3N\times 1}$ and $U = [u_1, u_2, \ldots, u_N]^T \in \mathbb{R}^{N\times 1}$ for the N followers. Then, we have the collective dynamics of nodes from 1 to N is

$$\dot{X} = I_N \otimes A \cdot X + I_N \otimes B \cdot U \tag{12}$$

with $I_N \otimes A \in \mathbb{R}^{3N\times 3N}$, $I_N \otimes B \in \mathbb{R}^{3N\times N}$. By (11), the control law governed by G is

$$U = -\mathcal{K}^T(G) \cdot X \tag{13}$$

with $\mathcal{K}(G) = \{\mathcal{k}_{i,j}\} \in \mathbb{R}^{3N\times N}$, defined as

$$\mathcal{k}_{ij} = \begin{cases} -a_{ij} \cdot k_{ij}, & i \neq j \\ -\sum_{w=1, w\neq i}^{N} \mathcal{k}_{iw} + p_i k_{i0}, & i = j \end{cases} \tag{14}$$

where $\mathcal{k}_{ij} \in \mathbb{R}^{3\times 1}$, $i, j = 1, \ldots, N$. Substituting (13) into (12), the closed-loop dynamics of the homogeneous platoon are

$$\dot{X} = \{I_N \otimes A - I_N \otimes B \cdot \mathcal{K}^T(G)\} \cdot X. \tag{15}$$

The closed-loop dynamics are a function of four components: 1) vehicle longitudinal dynamics, represented by A and B; 2) information flow topology, represented by G; 3) decentralized control law, represented by $\mathcal{K}(G)$; and 4) geometry formation, included in X as the desired distance [see (10)]. Note that $\mathcal{K}(G)$ is structured, governed by information flow topology G and control gain k_{ij}. In this paper, we focus on the information flow topology G and control gain k_{ij} to study the scalability limitation of large-scale platoons.

1) Closed-Loop Dynamics for Platoon Under UIF Topology With Linear Identical Controllers: A platoon is said to be under UIF topology if G is undirected when restricted to the set of followers, i.e., $j \in \mathbb{N}_i \Leftrightarrow i \in \mathbb{N}_j$, $i, j = 1, 2, \ldots, N$. Under the UIF topology, we limit our discussion to linear identical controllers, i.e., $k_{ij} = k = [k_s, k_v, k_a]^T \in \mathbb{R}^{3\times 1}$, $i, j = 0, \ldots, N$. Then, $\mathcal{K}(G)$ is simplified to

$$\mathcal{K}(G) = -(\mathcal{L}_{\text{UIF}} + \mathcal{P}_{\text{UIF}}) \otimes k \tag{16}$$

where $\mathcal{L}_{\text{UIF}}$ and $\mathcal{P}_{\text{UIF}}$ are the $\mathcal{L}$ and $\mathcal{P}$ associated with the UIF topology, respectively. Therefore, the closed-loop dynamics for platoon under the UIF topology with linear identical controllers become

$$\dot{X} = A_{c,\text{UIF}} \cdot X \tag{17}$$

where $A_{c,\text{UIF}} \in \mathbb{R}^{3N\times 3N}$, defined as

$$A_{c,\text{UIF}} = I_N \otimes A - (\mathcal{L}_{\text{UIF}} + \mathcal{P}_{\text{UIF}}) \otimes Bk^T. \tag{18}$$

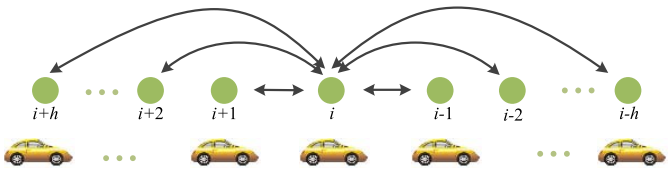

Fig. 2. Definition of h-neighbor UIF topology.

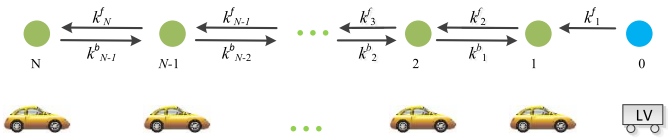

Fig. 3. Platoon under the BD topology.

In fact, the UIF topology includes a large class of topologies. One most commonly used variant is the h-neighbor UIF topology, as shown in Fig. 2.

Definition 1 (h-Neighbor UIF Topology): The information flow topology is said to be an h-neighbor UIF topology, if each follower can reach its nearest h neighbors in the set of followers, i.e., $\mathbb{N}_i = \{i-h, \ldots, i+h\} \cap \{1, \ldots, N\} \backslash \{i\}$, no matter how many followers are pinned to the leader.

In the h-neighbor UIF topology, h represents the range of reliable wireless communication. This topology is said to be strong connected if $h = N-1$, i.e., every follower can reach all the other followers.

2) Closed-Loop Dynamics for Platoon Under BD Topology With Linear Asymmetric Controller: Another focus of this paper is the asymmetric control, which has been revealed to be beneficial for scalability. For asymmetric control, only the BD topology is discussed for simplicity. Under the BD topology, decentralized controllers can only receive the information from its nearest, i.e., front and back, neighbors, as shown in Fig. 3.

Under the BD topology, the linear control law (11) is specified as

$$\begin{cases} u_i(t) = -\left(k_i^f\right)^T(\tilde{x}_i - \tilde{x}_{i-1}) - \left(k_i^b\right)^T(\tilde{x}_i - \tilde{x}_{i+1}), \\ \qquad\qquad\qquad\qquad\qquad i = 1, \ldots, N-1 \\ u_N(t) = -\left(k_N^f\right)^T(\tilde{x}_N - \tilde{x}_{N-1}) \end{cases} \tag{19}$$

where $k_i^f = [k_{i,s}^f, k_{i,v}^f, k_{i,a}^f]^T \in \mathbb{R}^{3\times 1}$ is the control gain for the front node and $k_i^b = [k_{i,s}^b, k_{i,v}^b, k_{i,a}^b]^T \in \mathbb{R}^{3\times 1}$ is the control gain for the back node.

Definition 2 (Asymmetric Control): The controller is called asymmetric, if

$$\begin{cases} k_i^f = (1+\epsilon)k, \quad k_i^b = (1-\epsilon)k \quad i = 1, \ldots, N-1 \\ k_N^f = (1+\epsilon)k \end{cases} \tag{20}$$

where $\epsilon \in (0, 1)$ is called the asymmetric degree. Note that if $\epsilon = 0$, then (20) is reduced to the symmetric case. The definition above reduces $\mathcal{K}(G)$ into

$$\mathcal{K}^T(G) = (\mathcal{L}_{\mathrm{BD}} + \mathcal{P}_{\mathrm{BD}})_\epsilon \otimes k^T \tag{21}$$

where $(\mathcal{L}_{\mathrm{BD}} + \mathcal{P}_{\mathrm{BD}})_\epsilon$ incorporates the $\mathcal{L} + \mathcal{P}$ associated with the BD topology and the asymmetric degree ϵ

$$(\mathcal{L}_{\mathrm{BD}} + \mathcal{P}_{\mathrm{BD}})_\epsilon = \begin{bmatrix} 2 & -1+\epsilon & & & \\ -1-\epsilon & 2 & -1+\epsilon & & \\ & \ddots & \ddots & \ddots & \\ & & -1-\epsilon & 2 & -1+\epsilon \\ & & & -1-\epsilon & 1+\epsilon \end{bmatrix}. \tag{22}$$

Therefore, the closed-loop dynamics for platoon under the BD topology with linear asymmetric controllers become

$$\dot{X} = A_{c,\mathrm{BD}} \cdot X \tag{23}$$

where $A_{c,\mathrm{BD}} \in \mathbb{R}^{3N\times 3N}$, defined as

$$A_{c,\mathrm{BD}} = I_N \otimes A - (\mathcal{L}_{\mathrm{BD}} + \mathcal{P}_{\mathrm{BD}})_\epsilon \otimes Bk^T. \tag{24}$$

III. Methods to Improve the Stability Margin

This section focuses on the stability margin analysis of homogeneous platoons moving in a rigid formation. We first need to clarify the definitions of stability, scalability, and stability margin of a platoon.

Definition 3 (Stability): A platoon with linear time invariant dynamics is said to be stable if the closed-loop system has eigenvalues with strictly negative real parts, i.e., in the open left half of the complex plane [28], [29].

Definition 4 (Scalability): A platoon is said to be scalable, if all the stable closed-loop eigenvalues are bound away from zero and independent of the platoon size [29].

Definition 5 (Stability Margin): The stability margin of a platoon is defined as the absolute value of the real part of the least stable eigenvalue [26], [28].

In this section, two theorems will be proved for homogeneous platoons both under the UIF topology with identical controllers and under the BD topology with asymmetric controllers. These two theorems point out the scalability limitation of large-scale platoons, and provide two basic ways to improve the stability margin, i.e., enlarging information topology and employing asymmetric control.

A. Stability and Scalability of Platoon Under UIF Topology With Linear Identical Controllers

Before we present the first theorem, we need the following lemmas.

Lemma 1 [32]: For any information flow topology, all the eigenvalues of $\mathcal{L}$ have nonnegative real parts, i.e., $\mathrm{Re}[\sigma_i(\mathcal{L})] \geq 0$, $i = 1, 2, \ldots, N$. Zero is an eigenvalue of $\mathcal{L}$, with $\mathbf{1_N} = [1, 1, \ldots, 1]^T \in \mathbb{R}^{N\times 1}$ as the corresponding eigenvector, i.e., $\mathcal{L} \cdot \mathbf{1_N} = \mathbf{0}$.

Lemma 2 [35], [36]: All the eigenvalues of $\mathcal{L} + \mathcal{P}$ are located in the open right half plane, i.e., $\mathrm{Re}[\sigma_i(\mathcal{L} + \mathcal{P})] > 0$, $i = 1, 2, \ldots, N$, when graph G contains a spanning tree rooting from the leader.

Lemma 3 [34]: Let a symmetric matrix $Q = Q^T = [q_{ij}] \in \mathbb{R}^{n\times n}$ and $x \in \mathbb{R}^{n\times 1}$. Then, we have

$$\sigma_{\max}(Q) = \max_{x\neq 0} \frac{x^T Q x}{x^T x}, \quad \sigma_{\min}(Q) = \min_{x\neq 0} \frac{x^T Q x}{x^T x}.$$

This is the well-known Rayleigh–Ritz theorem.

Lemma 4 [35]: Given a real polynomial

$$p(s,\lambda) = s^3 + \frac{\lambda k_3 + 1}{\tau}s^2 + \lambda\frac{k_2}{\tau}s + \lambda\frac{k_1}{\tau} \tag{25}$$

where s denotes the independent variable, k_1, k_2, k_3, and τ are nonzero constant real numbers, and $\lambda \in \mathbb{R}$. If (25) is asymptotically stable, then it has the following.

1) Equation (25) has one characteristic root approaching $-1/\tau$ and two characteristic roots approaching zero with rate $O(\lambda)$ when λ goes to zero.
2) Equation (25) has no characteristic roots close to zero (or imaginary axis) unless λ is close to zero.

The first theorem of this paper is stated as follows.

Theorem 1: Consider a homogeneous platoon under the UIF topology with linear identical controllers given by (17).

1) Platoon (17) is asymptotically stable if and only if
$$\begin{cases} k_s > 0 \\ k_v > k_s\tau / \min\limits_{i\in\{1,\dots,N\}}(\lambda_i k_a + 1) \\ k_a > -1 / \max\limits_{i\in\{1,\dots,N\}}(\lambda_i) \end{cases} \tag{26}$$
where λ_i is the ith eigenvalue of $\mathcal{L}_{\rm UIF} + \mathcal{P}_{\rm UIF}$.
2) The stability margin for platoon (17) decays to zero as the platoon size N increases, unless there exists a large number of followers, i.e., $O(N)$, that are pinned to the leader.

Proof: By Lemma 2, $\mathrm{Re}\{\lambda_i\} > 0$. From Definitions 6 and 7, we know that $\mathcal{L}_{\rm UIF}$ is symmetric, i.e., $\mathcal{L}_{\rm UIF}^T = \mathcal{L}_{\rm UIF}$, and $\mathcal{P}_{\rm UIF}$ is a diagonal matrix. Hence, $\mathcal{L}_{\rm UIF} + \mathcal{P}_{\rm UIF}$ is also symmetric, indicating $\lambda_i \in \mathbb{R}$, $i = 1, 2, \dots, N$.

As a result, there exists a unitary matrix W such that

$$W^{-1} \cdot (\mathcal{L}_{\rm UIF} + \mathcal{P}_{\rm UIF}) \cdot W = \Lambda_{\rm UIF} \tag{27}$$

where $\Lambda_{\rm UIF} \in \mathbb{R}^{N\times N}$ is a diagonal matrix with the eigenvalues of $\mathcal{L}_{\rm UIF} + \mathcal{P}_{\rm UIF}$ being the diagonal entries

$$\Lambda_{\rm UIF} = \begin{bmatrix} \lambda_{\min} & & & \\ & \lambda_2 & & \\ & & \ddots & \\ & & & \lambda_{\max} \end{bmatrix}.$$

Then, the similarity transformation of $A_{c,\rm UIF}$ gives a block triangular matrix

$$\begin{aligned} \tilde{A}_{c,\rm UIF} &= (W \otimes I_N)^{-1} \cdot A_{c,\rm UIF} \cdot (W \otimes I_N) \\ &= (W \otimes I_N)^{-1} \cdot (I_N \otimes A - (L_{\rm UIF} + P_{\rm UIF}) \otimes Bk^T) \\ &\quad \cdot (W \otimes I_N) = I_N \otimes A - \Lambda_{\rm UIF} \otimes Bk^T \end{aligned} \tag{28}$$

which leads to

$$S(A_{c,\rm UIF}) = S(\tilde{A}_{c,\rm UIF}) = \bigcup_{i=1}^{N}\{S(A - \lambda_i Bk^T)\}. \tag{29}$$

Therefore, platoon (17) is asymptotically stable if and only if $A - \lambda_i Bk^T$, $i = 1, 2, \dots, N$ are all Hurwitz. The characteristic polynomial of matrix $A - \lambda_i Bk^T$ is

$$|sI - (A - \lambda_i Bk^T)| = s^3 + \frac{\lambda_i k_a + 1}{\tau}s^2 + \frac{\lambda_i k_v}{\tau}s + \frac{\lambda_i k_s}{\tau}. \tag{30}$$

The stability of (30) is examined using the Routh–Hurwitz stability criterion, shown in

$$\begin{array}{ll} s^3 & 1 \qquad\qquad\qquad\qquad\qquad\qquad \dfrac{\lambda_i k_v}{\tau} \\ s^2 & \dfrac{\lambda_i k_a + 1}{\tau} \qquad\qquad\qquad\qquad \dfrac{\lambda_i k_s}{\tau} \\ s^1 & \dfrac{\lambda_i k_v(\lambda_i k_a + 1) - \lambda_i k_s \tau}{\tau(\lambda_i k_a + 1)} \\ s^0 & \dfrac{\lambda_i k_s}{\tau}. \end{array} \tag{31}$$

Given the fact $\tau > 0$, $\lambda_i > 0$, $i = 1, 2, \dots, N$, (30) is asymptotically stable if and only if

$$\begin{cases} k_s > 0 \\ k_v > k_s\tau/(\lambda_i k_a + 1), \quad i = 1, \dots, N \\ k_a > -1/\lambda_i. \end{cases} \tag{32}$$

Thus, platoon (17) is asymptotically stable if and only if (26) are satisfied.

To prove Theorem 1 (1.2), based on Lemma 3, we know

$$\lambda_{\min} \le \frac{x^T(L_{\rm UIF} + P_{\rm UIF})x}{x^T x} \quad \forall x \in \mathbb{R}^{N\times 1}. \tag{33}$$

Therefore, by choosing $x = \mathbf{1}_N \in \mathbb{R}^{N\times 1}$, we obtain

$$\lambda_{\min} \le \frac{x^T(L_{\rm UIF} + P_{\rm UIF})x}{x^T x} = \frac{x^T L_{\rm UIF} x + x^T P_{\rm UIF} x}{N}. \tag{34}$$

From the definition of pinning matrix (7), we have

$$x^T P_{\rm UIF} x = \sum_{i=1}^{N} p_i = \Omega(N) \tag{35}$$

where $\Omega(N)$ denotes the number of followers that are pinned to the leader. Hence, based on Lemma 1, the upper and lower bounds for the least eigenvalue of $\mathcal{L}_{\rm UIF} + \mathcal{P}_{\rm UIF}$ are given by

$$0 < \lambda_{\min} \le \frac{x^T L_{\rm UIF} x + x^T P_{\rm UIF} x}{N} = \frac{\Omega(N)}{N}. \tag{36}$$

If there are not enough followers connected to the leader, i.e., $\Omega(N)$ is independent of the platoon size N, then we have

$$\forall \varepsilon > 0, \quad \exists N > 0, \quad \text{s.t.,} \ \frac{\Omega(N)}{N} < \varepsilon. \tag{37}$$

Based on (36) and (37), we know that $\lambda_{\min}$ can be sufficiently close to zero as the platoon size N become sufficiently large (note N can also be a finite number). Based on Lemma 4, two characteristic roots of $A - \lambda_{\min} Bk^T$ approach zero as $\lambda_{\min}$ goes to zero. Under this circumstance, the stability margin for platoon (17) decays to zero as the platoon size N becomes sufficiently large.

If the number of followers connected to the leader satisfies

$$\frac{\Omega(N)}{N} = \text{const} \in (0, 1] \Rightarrow \Omega(N) = O(N) \tag{38}$$

it is possible that the stability margin for platoon (17) does not decay to zero as the size of platoon increases, which implies that the scalability of platoon (17) may be guaranteed. ■

Remark 1: Theorem 1 (1.2) explicitly establishes the stabilization thresholds of linear control gains for platoons with

the UIF topology. The similarity transformation in (28) actually decomposes a platoon (17) into multiple subsystems. This kind of technique originated in [8], has been used in [22], [24], [28], [29], and [36].

Remark 2: Theorem 1 (1.2) demonstrates the scalability limitation of a platoon under the UIF topology with linear identical controllers. This conclusion agrees with [9], and [24], in which the vehicle dynamic was assumed to be a double integrator. Our research extends their results in [9] [24] by taking into account the inertial lag in vehicle longitudinal dynamics.

Remark 3: Theorem 1 (1.2) implies that the information from the leader is more important than that among the followers. Even though the topology among the followers is strongly connected, the scalability of platoon (17) cannot be guaranteed unless enough followers are pinned to the leader. Intuitively, the information flow among the followers may help to regulate the local spacing errors. However, the ultimate goal for a large-scale platoon is to track the leader. Hence, enough followers pinned to the leader are required to guarantee scalability.

Remark 4: If every follower can reach the leader, resulting in the topologies like the BD-leader (BDL) topology, i.e., $\Omega(N) = N$. It is known that the BDL topology is scalable [7], [35]. Some topologies like the BD topology ($\Omega(N) = 1$) suffers from the fundamental limitation that the stability margin decays to zero as the platoon size increases [7], [21], [22], [35].

Remark 5: Theorem 1 (1.1) is a necessary and sufficient condition for the closed-loop stability, while Theorem 1 (1.2) is only necessary for scalability. Even though the number of followers pinned to the leader is $\Omega(N) = O(N)$, the stability margin may still decay to zero as the platoon size increases. We argue that to obtain a scalable platoon, the tree depth of graph G should be a constant and independent of the platoon size N. Note that, the tree depth in this paper is defined as follows (which is different from the typical definition in [32]).

Definition 6: Tree depth c is defined as

$$c = \max\{n_1, n_2 - n_1, \ldots, n_p - n_{p-1}, N - n_p + 1\} \quad (39)$$

where $\{n_1, n_2, \ldots, n_p\}$, $1 \le n_1 \le \cdots \le n_p \le N$ is the set of followers pinned to the leader.

Fig. 4 demonstrates the two UIF topologies. The simulations in Section IV-A show that one of them [Fig. 4(a), $\Omega(N) = O(N), c = N/2$] will lose the stability margin as the platoon size increases, and the other one [Fig. 4(b), $\Omega(N) = O(N)$ and c is a constant] is scalable.

B. Scalability of Platoon Under BD Topology With Asymmetric Control

Theorem 1 highlights the importance of topology selection to the platoon scalability. Enough followers are required to be pinned to the leader, but at the expense of a large amount of communication. Asymmetric controllers have also attracted extensive attention for its potential to reduce the loss of stability margin as the platoon size increases [26], [28], [29]. This section focuses on a special UIF topology, i.e., the BD

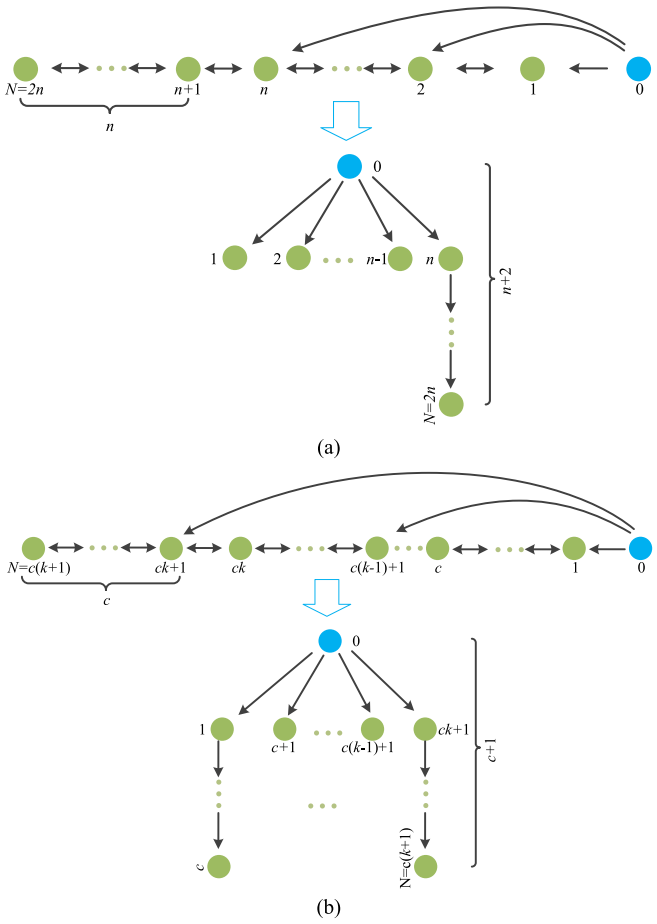

Fig. 4. Platoon with a large number of followers pinned to the leader. (a) UIF topology contains a spanning tree with a tree depth that is of the same order as N. (b) UIF topology contains a spanning tree with a constant tree depth c, which is independent of the platoon size N.

topology (see Fig. 3), to demonstrate how to select asymmetry decentralized controllers. Before presenting the second theorem, the following lemmas are needed.

Lemma 5 [32]: Suppose that

$$\tilde{D} = \begin{bmatrix} D & y \\ y^T & d_n \end{bmatrix} \in \mathbb{R}^{n\times n}$$

is a symmetric matrix and D is a $(n-1)$-by-$(n-1)$ symmetric matrix. Let $\gamma_1 \le \gamma_2 \le \cdots \le \gamma_n$ be the eigenvalues of $\tilde{D}$ and $\beta_1 \le \beta_2 \le \cdots \le \beta_{n-1}$ be the eigenvalues of D. Then

$$\gamma_1 \le \beta_1 \le \cdots \le \beta_{i-1} \le \gamma_i \le \beta_i \le \gamma_{i+1} \le \cdots \le \beta_{n-1} \le \gamma_n. \quad (40)$$

Lemma 6 [34]: Let a matrix $Q = [q_{ij}] \in \mathbb{R}^{n\times n}$. Then, all the eigenvalues of Q are located in the union of the n disks

$$\bigcup_{i=1}^{n} \left\{ \lambda \in \mathbb{C} \| \lambda - q_{ii}| \le \sum_{j=1, j\ne i}^{n} |q_{ij}| \right\}.$$

Note that, Lemma 5 is the well-known Cauchy Interlace Theorem, and Lemma 6 is the Geršgorin Disk Criterion.

The following proposition is derived for comparison.

Proposition 1 [35]: Consider a homogeneous platoon under the BD topology with symmetric controllers, and assume that

the controllers satisfy Theorem 1 (1.1). Then, the stability margin of the platoon decays to zero as $O(1/N^2)$.

Note that, Proposition 1 considers the inertial lag of powertrain dynamics in nodes. This proposition conforms to [26], and [29], in which the node dynamics are double integrators.

Theorem 2: Consider a homogeneous platoon under the BD topology with the asymmetric controller architecture given by (23).

1) Platoon (23) is asymptotically stable if and only if

$$\begin{cases} k_s > 0 \\ k_v > k_s\tau / \min\limits_{i\in\{1,\dots,N\}}(\sigma_i(\mathcal{LP}_\epsilon)k_a + 1) \\ k_a > -1/\max\limits_{i\in\{1,\dots,N\}}(\sigma_i(\mathcal{LP}_\epsilon)) \end{cases} \tag{41}$$

where $\mathcal{LP}_\epsilon$ denotes $(L_{\mathrm{BD}} + P_{\mathrm{BD}})_\epsilon$ for simplicity in this section.

2) For any fixed $\epsilon \in (0, 1)$, the stability margin is bounded away from zero and independent of the platoon size N (N can be any finite integer).

Proof: To prove Theorem 2 (2.1), we note that $\mathcal{LP}_\epsilon$ in (22) is asymmetric. This matrix can be transformed into a symmetric matrix. Choose $S \in \mathbb{R}^{N\times N}$ as

$$S = \begin{bmatrix} 1 & & & \\ & \left(\frac{1-\epsilon}{1+\epsilon}\right)^{\frac{1}{2}} & & \\ & & \ddots & \\ & & & \left(\frac{1-\epsilon}{1+\epsilon}\right)^{\frac{N-1}{2}} \end{bmatrix}.$$

Then, we have

$$\begin{aligned} \widetilde{\mathcal{LP}}_\epsilon &= S(\mathcal{LP}_\epsilon)S^{-1} \\ &= \begin{bmatrix} 2 & -\delta & & & \\ -\delta & 2 & -\delta & & \\ & \ddots & \ddots & \ddots & \\ & & -\delta & 2 & -\delta \\ & & & -\delta & 1+\epsilon \end{bmatrix} \end{aligned} \tag{42}$$

where $\delta = \sqrt{(1-\epsilon)(1+\epsilon)}$. According to Lemma 6, all the eigenvalues of $\widetilde{\mathcal{LP}}_\epsilon$ are located in the union of two disks

$$\{\lambda \in \mathbb{C} || \lambda - 2| \le 2\delta\} \bigcup \{\lambda \in \mathbb{C} || \lambda - 1 - \epsilon| \le \delta\}. \tag{43}$$

It is easy to verify $2-2\delta > 0$, and $1+\epsilon-\delta > 0$, $\forall \epsilon \in (0, 1)$. Hence, $\sigma_i(\mathcal{LP}_\epsilon) = \sigma_i(\widetilde{\mathcal{LP}}_\epsilon) > 0$, $i = 1, 2, \dots, N$. Then, using similar techniques as in Theorem 1 (1.1), we have that platoon (23) is asymptotically stable if and only if (41) is satisfied.

The proof of Theorem 2 (2.2) proceeds in two steps.

Step 1: We first prove the upper and lower bounds of $\sigma_{\min}(\mathcal{LP}_\epsilon)$. In fact, $\widetilde{\mathcal{LP}}_\epsilon$ can be rewritten as

$$\widetilde{\mathcal{LP}}_\epsilon = \begin{bmatrix} Z & -e \\ -e^T & 1+\epsilon \end{bmatrix} \tag{44}$$

where $Z \in \mathbb{R}^{(N-1)\times(N-1)}$, $e \in \mathbb{R}^{(N-1)\times 1}$ are defined as

$$Z = \begin{bmatrix} 2 & -\delta & & & \\ -\delta & 2 & -\delta & & \\ & -\delta & 2 & \ddots & \\ & & \ddots & \ddots & -\delta \\ & & & -\delta & 2 \end{bmatrix}, \quad e = \begin{bmatrix} 0 \\ 0 \\ \vdots \\ \delta \end{bmatrix}.$$

Further, Z is decomposed to $Z = 2I_{N-1} - \delta \cdot H$, where $H \in \mathbb{R}^{(N-1)\times(N-1)}$ is defined as

$$H = \begin{bmatrix} 0 & 1 & & & \\ 1 & 0 & 1 & & \\ & 1 & 0 & \ddots & \\ & & \ddots & \ddots & 1 \\ & & & 1 & 0 \end{bmatrix}.$$

It is known from [34] that the eigenvalues of matrix H are

$$\sigma_{N-i}(H) = 2\cos\frac{i\pi}{N}, \quad i = 1, \dots, N-1.$$

Then, the eigenvalues of Z are

$$\sigma_i(Z) = 2 - 2\delta\cos\frac{i\pi}{N}, \quad i = 1, \dots, N-1. \tag{45}$$

By Lemma 5, we have

$$\sigma_{\min}(\widetilde{\mathcal{LP}}_\epsilon) \le \sigma_{\min}(Z) = 2 - 2\delta\cos\frac{\pi}{N}. \tag{46}$$

Equation (46) actually gives the upper bound of $\sigma_{\min}(\widetilde{\mathcal{LP}}_\epsilon)$. To obtain the lower bound of $\sigma_{\min}(\widetilde{\mathcal{LP}}_\epsilon)$, we define

$$\begin{aligned} Y &= (\widetilde{\mathcal{LP}}_\epsilon) - \epsilon^2 I_N \\ &= \begin{bmatrix} 2-\epsilon^2 & -\delta & & & \\ -\delta & 2-\epsilon^2 & -\delta & & \\ & \ddots & \ddots & \ddots & \\ & & -\delta & 2-\epsilon^2 & -\delta \\ & & & -\delta & 1+\epsilon-\epsilon^2 \end{bmatrix}. \end{aligned} \tag{47}$$

It is easy to know

$$1 - \frac{1}{2}\epsilon^2 \ge (1-\epsilon^2)^{\frac{1}{2}} = \delta \quad \forall \epsilon \in (0, 1). \tag{48}$$

Hence, we have

$$\begin{cases} 2 - \epsilon^2 - 2\delta \ge 2 - \epsilon^2 - 2\left(1 - \frac{1}{2}\epsilon^2\right) = 0 \\ 1 + \epsilon - \epsilon^2 - \delta \ge 1 + \epsilon - \epsilon^2 - \left(1 - \frac{1}{2}\epsilon^2\right) > 0 \\ \qquad\qquad\qquad\qquad\qquad\qquad \forall \epsilon \in (0, 1). \end{cases} \tag{49}$$

According to Lemma 6, and noting that Y is symmetric, all the eigenvalues of Y are real and nonnegative

$$\sigma_i(Y) \ge 0, \quad i = 1, 2, \dots, N.$$

Considering the definition (47) of Y, we have

$$\sigma_{\min}(\widetilde{\mathcal{LP}}_\epsilon) = \sigma_{\min}(Y) + \epsilon^2 \ge \epsilon^2. \tag{50}$$

Based on (42), (46), and (50), we claim that all the eigenvalues of $\mathcal{LP}_\epsilon$ are real and $\sigma_{\min}(\mathcal{LP}_\epsilon)$ will not decay to zero as the platoon size N increases

$$2-2\sqrt{1-\epsilon^2}\cos\frac{\pi}{N} \geq \sigma_{\min}(\mathcal{LP}_\epsilon) \geq \epsilon^2. \tag{51}$$

Note the basis matrix S is invertible for any finite integer N. Thus, (51) gives the upper and lower bounds of $\sigma_{\min}(\mathcal{LP}_\epsilon)$ for any finite integer N.

Step 2: We then prove that the stability margin is bounded away from zero and independent of the platoon size N. Using the similarity transformation as (28), we have that the spectrum of $A_{c,\mathrm{BD}}$ is expressed as

$$\begin{aligned} S(A_{c,\mathrm{BD}}) &= S(I_N \otimes A - \mathcal{LP}_\epsilon \otimes Bk^T) \\ &= \bigcup_{i=1}^{N} \{S(A-\sigma_i(\mathcal{LP}_\epsilon)Bk^T)\}. \end{aligned} \tag{52}$$

The characteristic polynomial of matrix $A-\sigma_i(\mathcal{LP}_\epsilon)Bk^T$ is

$$\begin{aligned} &|sI-(A-\sigma_i(\mathcal{LP}_\epsilon)Bk^T)| \\ &= s^3 + \frac{\sigma_i(\mathcal{LP}_\epsilon)k_a+1}{\tau}s^2 + \frac{\sigma_i(\mathcal{LP}_\epsilon)k_v}{\tau}s + \frac{\sigma_i(\mathcal{LP}_\epsilon)k_s}{\tau}. \end{aligned} \tag{53}$$

According to (51), for any fixed $\epsilon \in (0,1)$ and any finite integer N, we have $\sigma_i(\mathcal{LP}_\epsilon) \geq \sigma_{\min}(\mathcal{LP}_\epsilon) \geq \epsilon^2$, which means $\sigma_i(\mathcal{LP}_\epsilon)$ is bounded away from zero. Based on Lemma 4, the eigenvalues of (53) are also bounded away from zero. Therefore, there is a constant gap between the least stable closed-loop eigenvalue and the imaginary axis. Moreover, this gap is independent of the platoon size N (N can be any finite integer), i.e., the stability margin is bounded away from zero and independent of the platoon size N. ■

Remark 6: Compared with Proposition 1, Theorem 2 (2.2) suggests that asymmetric control can significantly improve the stability margin of large-scale platoons, which hints that the controller structure may play a more important role than the feedback gain design.

Remark 7: Theorem 2 (2.2) shows that the asymmetric control architecture provides another way to obtain scalable platoons. This finding conforms to the results in [26] and [28], which adopted the PDE approximation and were only suitable for vanishingly small asymmetric structures. This paper proves the main results using the matrix-based analysis without any approximation, and as a result provides more accurate prediction and can be used for large asymmetric control. In addition, our finding is an extension to [29], in which the dynamics of each node were assumed to be double integrators.

Remark 8: Conditions (26) and (41) need to know the spectrum of the Laplacian and pinning matrices, which is unfortunately not readily computable in a distributed way. However, we can still have some information about the distribution of eigenvalues provided that we have certain priori information on the topology. Thus, conditions (26) and (41) can provide a general guideline for designers to choose the controller gains. In addition, there exist some efforts to estimate the eigenvalues or even reconstruct the network topology in a distributed sense (see [37], [38]).

TABLE I
PARAMETERS IN SIMULATIONS

Parameters	Notation	Value
Inertial lag of vehicle longitudinal dynamics (s)	τ	0.5
Controller gains	k_s	1
	k_v	2
	k_a	1
Desired spacing (m)	$d_{i-1,i}$	20
Initial position of leader (m)	s_0	0
Initial speed of leader (m/s)	v_0	20
Initial spacing errors (m)	$\varepsilon_{s,i}$	0
Initial speed errors (m/s)	$\varepsilon_{v,i}$	0

Note: $\varepsilon_{s,i} = s_{i-1} - s_i - d_{i-1,i}$, and $\varepsilon_{v,i} = v_{i-1} - v_i$

IV. SIMULATION RESULTS AND DISCUSSION

Numerical simulations with a platoon of passenger cars are conducted to verify the main results in this paper. In the following simulations, the parameters, including the inertial lag, controller gains, and initial states are shown in Table I. For platoons under the UIF topology, the controller gains shown in Table I satisfy Theorems 1 (1.1) and 2 (2.1). Thus, the closed-loop stability is always ensured. The acceleration or deceleration of the leader can be viewed as the disturbance to the platoon. The leader is set to run along

$$v_0 = \begin{cases} 20 \text{ m/s} & t \leq 5 \text{ s} \\ 20+2t \text{ m/s} & 5 \text{ s} < t \leq 10 \text{ s} \\ 30 \text{ m/s} & t > 10 \text{ s}. \end{cases}$$

In this section, we demonstrate both the stability margin and transient performance for platoons under different UIF topologies. The transient performance corresponds to the aforementioned scenario: the leader's speed changes from one steady value to another, then we observe the state tracking errors of the followers during the transient process.

The stability margin is used to characterize the platoon scalability. The measure of transient performance is defined in (54)–(56), as suggested in [39].

Definition 7: Global transient performance index

$$E_g = \lim_{T\to\infty} \frac{1}{N}\sum_{i=1}^{N}\int_0^T \frac{1}{2}\left(\tilde{x}_i-\tilde{x}_{i-1}\right)^T R\left(\tilde{x}_i-\tilde{x}_{i-1}\right) \tag{54}$$

where $R = \mathrm{diag}\{k_s, k_v, k_a\}$ represents that the control gains are used as the weighting factors. E_g can reflect the global tracking performance during the transient process. We also define the local tracking performance by disregarding the tracking error with respect to the leader.

Definition 8: Local transient performance index

$$E_l = \lim_{T\to\infty} \frac{1}{N-1}\sum_{i=2}^{N}\int_0^T \frac{1}{2}(\tilde{x}_i-\tilde{x}_{i-1})^T R(\tilde{x}_i-\tilde{x}_{i-1}). \tag{55}$$

An index called convergence performance index is defined to characterize the settling time, i.e., the minimum time after which the state error becomes sufficiently small.

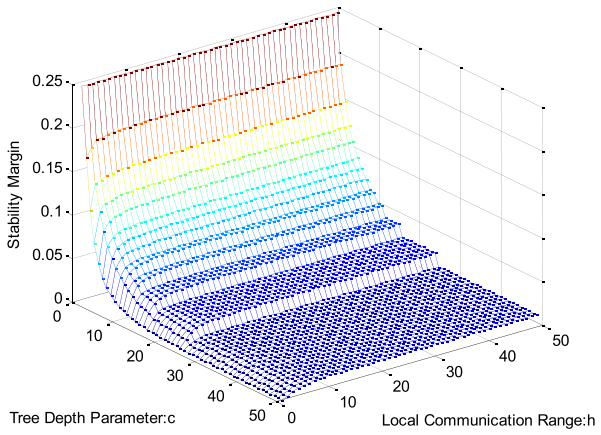

Fig. 5. Stability margin for a platoon under UIF topology with different tree depths c and local communication range h.

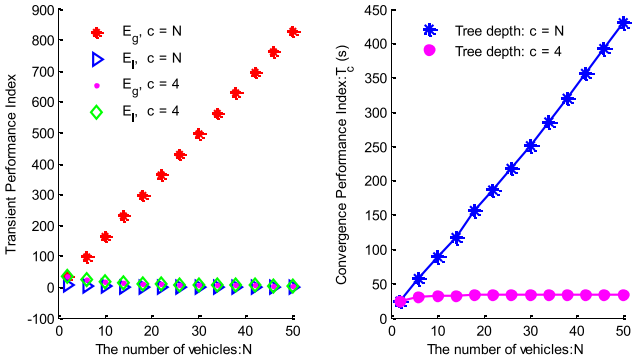

Fig. 6. Comparison of E_g, E_l, and T_c for a platoon under strong connected UIF topology with different sizes N and tree depths c.

Definition 8: Convergence performance index

$$T_c = \min_{T_1} \left(\max_{i=\{1,\ldots,N\}, t>T_1} |\varepsilon_{s,i}| < \delta \right). \tag{56}$$

In numerical simulations, the parameter T in (54) and (55) is chosen to be sufficiently large such that all the errors die out ($T = 2 \times 10^3$ s for computation). Parameter δ in (56) is set as $\delta = 0.1$ m.

A. Simulations for Platoon Under UIF Topology With Linear Identical Controllers

To demonstrate the influence of tree depth c and local communication range h on the stability margin of platoon (17), we fix the platoon size to be $N = 50$. As shown in Fig. 5, we can obviously observe that it is the tree depth c rather than local communication range h that dominates the scaling trend of the stability margin. Even though the information flow topology among the followers is strongly connected (i.e., $h = 49$ in this case), the stability margin is still close to zero, unless enough followers are pinned to the leader (i.e., small tree depth c). This result confirms Theorem 1 (1.2).

To demonstrate the scaling trend of performance indexes (i.e., E_g, E_l, T_c) for platoons under a strongly connected topology with two different tree depths (one is constant, i.e., $c = 4$, and the other is of the same order as the platoon size, i.e., $c = N$), we vary the platoon size N from 4 to 50. As shown in Fig. 6, the tracking errors among the followers (see E_l in Fig. 6) during the transient process in all cases are close to zero and the corresponding scaling trend is very well.

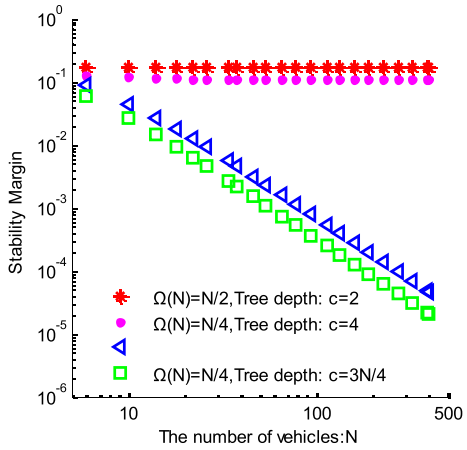

Fig. 7. Stability margin for UIF topology with different numbers of followers pinned to the leader and different tree depths (see the topology shown in Fig. 4).

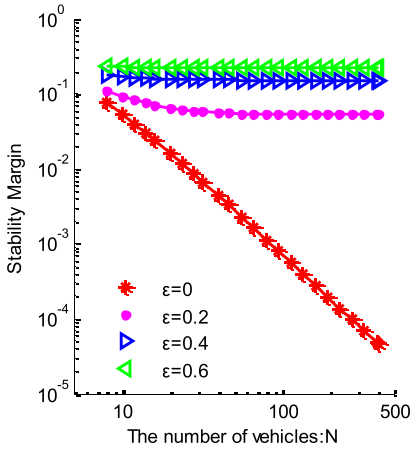

Fig. 8. Stability margin for BD topology with different asymmetric degrees (see the topology in Fig. 3).

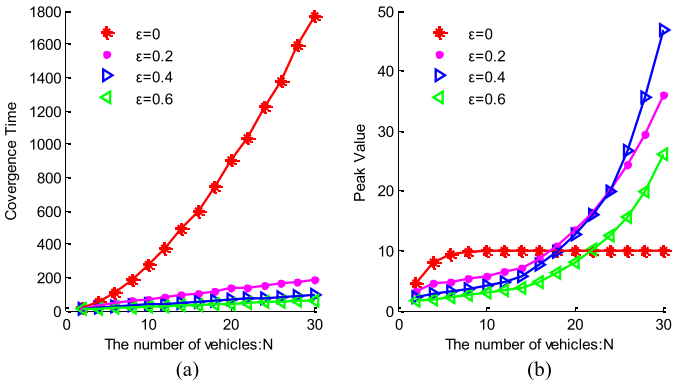

Fig. 9. Performance of a platoon under BD topology with symmetric and asymmetric controllers. (a) Convergence time. (b) Peak value.

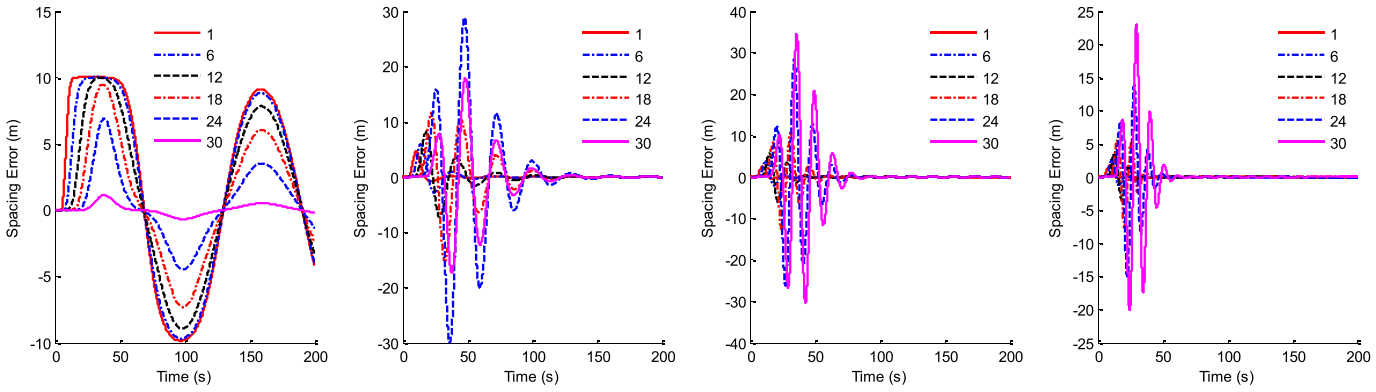

Fig. 10. Space errors for a homogeneous platoon under BD topology with different asymmetric degrees ϵ. (a) $\epsilon = 0$ (symmetric). (b) $\epsilon = 0.2$. (c) $\epsilon = 0.4$. (d) $\epsilon = 0.6$.

Actually, in simulations, we have seen that the platoon looks like one enlarged follower in tracking the leader's trajectory, indicating that the platoon under the strongly connected UIF topology can quickly regulate local spacing errors. However, if only the first follower is pinned to the leader (i.e., tree depth $c = N$), then the scaling trend of the global transient performance index E_g becomes worse. Actually, in simulations, we have seen that the first follower's spacing error oscillates larger, and convergence becomes slower as the platoon size increases, indicating that the information flow among the followers is beneficial for regulating local behavior (good for local safety), but does not contribute to the scalability of large platoons. Meanwhile, if there is one follower that can obtain the leader's information every four followers (i.e., tree depth $c = 4$), then the scalability performance is significantly improved.

Fig. 7 corroborates the statements in Remark 5 that even though $\Omega(N) = O(N)$, the stability margin may still decay to zero as the platoon size increases. The simulation results in Figs. 6 and 7 demonstrate that ensuring a constant tree depth in the UIF topology, platoon scalability can be guaranteed.

B. Simulations for Platoon Under BD Topology With Linear Asymmetric Controller

As shown in Fig. 8, the stability margin of the platoon with asymmetric controllers is indeed bounded away from zero and independent of with the platoon size, which confirms to Theorem 2 (2.2). To demonstrate the scaling trend of performance indexes for a platoon under the BD topology with different asymmetric degrees (i.e., $\epsilon = 0, 0.2, 0.4, 0.6$), we vary the platoon size N from 2 to 30.

As shown in Fig. 9, the convergence time for the platoon with symmetric control, i.e., $\epsilon = 0$, becomes large as the platoon size increases, whereas the convergence time for the platoon with asymmetric control increases with a relatively lower magnitude. However, the asymmetric control also introduces large peak during the transient process.

Fig. 10 shows the spacing errors for the homogeneous platoon under the BD topology with different asymmetric degrees ϵ. It is assumed that there are 30 followers in the platoon, i.e., $N = 30$. The exponential stability and convergence speed have been improved a lot due to the asymmetric degree ϵ. However, asymmetric control indeed introduces large peak phenomena during the transient performance, which is detrimental to the local safety of the platoon.

The stability margin only characterizes the global stability and cannot guarantee the transient performance. Even though asymmetric control can bound the stability margin away from zero, for actual implementation of the platoon system, we should take the transient performance into account. How to balance these performance criterions need further research.

V. Conclusion

From the viewpoint of both the information flow topology and decentralized controllers, this paper studies the scalability limitation of a homogenous platoon moving in a rigid formation and provides two basic ways to obtain scalable platoon systems, i.e., enlarging information topology and employing asymmetric control. A third-order state-space model for vehicle longitudinal dynamics is first derived using feedback linearization, which accommodates the inertial lag of powertrain dynamics. Graph techniques are adopted to model the UIF topology among vehicles, including both radar and communication based. Linear identical decentralized controllers for general UIF topologies and asymmetric decentralized controllers for the BD topology are designed, leading to platoon closed-loop dynamics under constant distance policy. The main contributions are as follows.

1) The first main theorem explicitly establishes the stabilization thresholds of linear identical decentralized control gains for homogeneous platoons interconnected by UIF topologies using matrix theory and the Routh–Hurwitz stability criterion. Meanwhile, using the Rayleigh–Ritz theorem, it is pointed out that the stability margin of a platoon under the UIF topology will not decay to zero as the size of the platoon increases only if there are a large number of followers, i.e., $O(N)$, pinned to the leader, which means the information flow among followers do not contribute to the scalability of a platoon. Extending the information flow topology to reduce the tree depth is one major way to achieve scalable platoon systems.

2) The second main theorem shows the benefit of employing the asymmetric controller architecture and points out that the stability margin of a platoon under the BD topology with asymmetric control can be bounded away from zero and independent of the platoon size. Employing the asymmetric controller architecture is another way to obtain scalable platoon systems from the viewpoint of getting constant stability margins.

Topics for future research include studies about the influence of communication delay, packet loss, and heterogeneous dynamics on the stability margin. The robustness issue, like parametric and model uncertainty, is another important topic on the platoon control and worth further research. In addition, there is a need to extend the analysis to incorporate the transient performance into the asymmetric controller design.

ACKNOWLEDGMENT

The authors would like to thank Dr. D. Cao of the Cranfield University, U.K., for his suggestions on how to model and control vehicular platoon.

REFERENCES

[1] J. Zhang, F.-Y. Wang, K. Wang, W.-H. Lin, X. Xu, and C. Chen, "Data-driven intelligent transportation systems: A survey," *IEEE Trans. Intell. Transp. Syst.*, vol. 12, no. 4, pp. 1624–1639, Dec. 2011.

[2] D. Caveney, "Cooperative vehicular safety applications," *IEEE Control Syst.*, vol. 30, no. 4, pp. 38–53, Aug. 2010.

[3] J. Ploeg, N. van de Wouw, and H. Nijmeijer, "$\mathcal{L}_p$ string stability of cascaded systems: Application to vehicle platooning," *IEEE Trans. Control Syst. Technol.*, vol. 22, no. 2, pp. 786–793, Mar. 2014.

[4] S. E. Shladover *et al.*, "Automated vehicle control developments in the PATH program," *IEEE Trans. Veh. Technol.*, vol. 40, no. 1, pp. 114–130, Feb. 1991.

[5] D. Swaroop, J. K. Hedrick, C. C. Chien, and P. Ioannou, "A comparison of spacing and headway control laws for automatically controlled vehicles," *Vehicle Syst. Dyn., Int. J. Vehicle Mech. Mobility*, vol. 23, no. 1, pp. 597–625, 1994.

[6] J. Zhou and H. Peng, "Range policy of adaptive cruise control vehicles for improved flow stability and string stability," *IEEE Trans. Intell. Transp. Syst.*, vol. 6, no. 2, pp. 229–237, Jun. 2005.

[7] D. Swaroop and J. K. Hedrick, "Constant spacing strategies for platooning in automated highway systems," *J. Dyn. Syst., Meas., Control*, vol. 121, no. 3, pp. 462–470, 1999.

[8] J. A. Fax and R. M. Murray, "Information flow and cooperative control of vehicle formations," *IEEE Trans. Autom. Control*, vol. 49, no. 9, pp. 1465–1476, Sep. 2004.

[9] S. K. Yadlapalli, S. Darbha, and K. R. Rajagopal, "Information flow and its relation to stability of the motion of vehicles in a rigid formation," *IEEE Trans. Autom. Control*, vol. 51, no. 8, pp. 1315–1319, Aug. 2006.

[10] Y. Zheng, S. E. Li, J. Wang, L. Y. Wang, and K. Li, "Influence of information flow topology on closed-loop stability of vehicle platoon with rigid formation," in *Proc. IEEE 17th Int. Conf. Intell. Transp. Syst. Conf.*, Oct. 2014, pp. 2094–2100.

[11] L. Xiao and F. Cao, "Practical string stability of platoon of adaptive cruise control vehicles," *IEEE Trans. Intell. Transp. Syst.*, vol. 12, no. 4, pp. 1184–1194, Dec. 2011.

[12] R. Teo, D. M. Stipanovic, and C. J. Tomlin, "Decentralized spacing control of a string of multiple vehicles over lossy datalinks," *IEEE Trans. Control Syst. Technol.*, vol. 18, no. 2, pp. 469–473, Mar. 2010.

[13] E. Shaw and J. K. Hedrick, "String stability analysis for heterogeneous vehicle strings," in *Proc. Amer. Control Conf.*, Jul. 2007, pp. 3118–3125.

[14] C.-Y. Liang and H. Peng, "Optimal adaptive cruise control with guaranteed string stability," *Vehicle Syst. Dyn., Int. J. Vehicle Mech. Mobility*, vol. 32, nos. 4–5, pp. 313–330, 1999.

[15] S. S. Stankovic, M. J. Stanojevic, and D. D. Siljak, "Decentralized overlapping control of a platoon of vehicles," *IEEE Trans. Control Syst. Technol.*, vol. 8, no. 5, pp. 816–831, Sep. 2000.

[16] W. B. Dunbar and D. S. Caveney, "Distributed receding horizon control of vehicle platoons: Stability and string stability," *IEEE Trans. Autom. Control*, vol. 57, no. 3, pp. 620–633, Mar. 2012.

[17] R. Kianfar *et al.*, "Design and experimental validation of a cooperative driving system in the grand cooperative driving challenge," *IEEE Trans. Intell. Transp. Syst.*, vol. 13, no. 3, pp. 994–1007, Sep. 2012.

[18] T. Robinson, E. Chan, and E. Coelingh, "Operating platoons on public motorways: An introduction to the sartre platooning programme," in *Proc. 17th World Congr. Intell. Transp. Syst. (ITS)*, Oct. 2010, pp. 1–11.

[19] S. Tsugawa, S. Kato, and K. Aoki, "An automated truck platoon for energy saving," in *Proc. IEEE/RSJ Int. Conf. Intell. Robots Syst.*, San Francisco, CA, USA, Sep. 2011, pp. 4109–4114.

[20] S. E. Li, Y. Zheng, K. Li, and J. Wang, "An overview of vehicular platoon control under the four-component framework," in *Proc. IEEE Intell. Vehicles Symp.*, Seoul, Korea, Jun./Jul. 2015, pp. 286–291.

[21] P. Seiler, A. Pant, and K. Hedrick, "Disturbance propagation in vehicle strings," *IEEE Trans. Autom. Control*, vol. 49, no. 10, pp. 1835–1842, Oct. 2004.

[22] P. Barooah and J. P. Hespanha, "Error amplification and disturbance propagation in vehicle strings with decentralized linear control," in *Proc. 44th IEEE Conf. Decision Control, Eur. Control Conf.*, Dec. 2005, pp. 4964–4969.

[23] R. H. Middleton and J. H. Braslavsky, "String instability in classes of linear time invariant formation control with limited communication range," *IEEE Trans. Autom. Control*, vol. 55, no. 7, pp. 1519–1530, Jul. 2010.

[24] S. Darbha and P. R. Pagilla, "Limitations of employing undirected information flow graphs for the maintenance of rigid formations for heterogeneous vehicles," *Int. J. Eng. Sci.*, vol. 48, no. 11, pp. 1164–1178, 2010.

[25] B. Bamieh, M. R. Jovanovic, P. Mitra, and S. Patterson, "Coherence in large-scale networks: Dimension-dependent limitations of local feedback," *IEEE Trans. Autom. Control*, vol. 57, no. 9, pp. 2235–2249, Sep. 2012.

[26] P. Barooah, P. G. Mehta, and J. P. Hespanha, "Mistuning-based control design to improve closed-loop stability margin of vehicular platoons," *IEEE Trans. Autom. Control*, vol. 54, no. 9, pp. 2100–2113, Sep. 2009.

[27] F. Lin, M. Fardad, and M. R. Jovanović, "Optimal control of vehicular formations with nearest neighbor interactions," *IEEE Trans. Autom. Control*, vol. 57, no. 9, pp. 2203–2218, Sep. 2012.

[28] H. Hao, P. Barooah, and P. G. Mehta, "Stability margin scaling laws for distributed formation control as a function of network structure," *IEEE Trans. Autom. Control*, vol. 56, no. 4, pp. 923–929, Apr. 2011.

[29] H. Hao and P. Barooah, "On achieving size-independent stability margin of vehicular lattice formations with distributed control," *IEEE Trans. Autom. Control*, vol. 57, no. 10, pp. 2688–2694, Oct. 2012.

[30] S. Li, K. Li, R. Rajamani, and J. Wang, "Model predictive multi-objective vehicular adaptive cruise control," *IEEE Trans. Control Syst. Technol.*, vol. 19, no. 3, pp. 556–566, May 2011.

[31] J.-Q. Wang, S. E. Li, Y. Zheng, and X.-Y. Lu, "Longitudinal collision mitigation via coordinated braking of multiple vehicles using model predictive control," *Integr. Comput.-Aided Eng.*, vol. 22, no. 2, pp. 171–185, 2015.

[32] C. Godsil and G. Royle, *Algebraic Graph Theory*, vol. 207. New York, NY, USA: Springer-Verlag, 2001.

[33] W. Ren and R. W. Beard, "Consensus seeking in multiagent systems under dynamically changing interaction topologies," *IEEE Trans. Autom. Control*, vol. 50, no. 5, pp. 655–661, May 2005.

[34] J. W. Demmel, *Applied Numerical Linear Algebra*. Philadelphia, PA, USA: SIAM, 1997.

[35] Y. Zheng, S. E. Li, J. Wang, D. Cao, and K. Li, "Stability and scalability of homogeneous vehicular platoon: Study on the influence of information flow topologies," *IEEE Trans. Intell. Transp. Syst.*, to be published.

[36] F. L. Lewis, H. Zhang, K. Hengster-Movric, and A. Das, *Cooperative Control of Multi-Agent Systems: Optimal and Adaptive Design Approaches*. London, U.K.: Springer-Verlag, 2014.

[37] M. Franceschelli, A. Gasparri, A. Giua, and C. Seatzu, "Decentralized estimation of Laplacian eigenvalues in multi-agent systems," *Automatica*, vol. 49, no. 4, pp. 1031–1036, 2013.

[38] F. Morbidi and A. Y. Kibangou, "A distributed solution to the network reconstruction problem," *Syst. Control Lett.*, vol. 70, pp. 85–91, Aug. 2014.

[39] H. Hao and P. Barooah, "Stability and robustness of large platoons of vehicles with double-integrator models and nearest neighbor interaction," *Int. J. Robust Nonlinear Control*, vol. 23, no. 18, pp. 2097–2122, 2013.

Yang Zheng received the B.E. degree from Tsinghua University, Beijing, China, in 2013, where he is currently pursuing the master's degree in automotive engineering with the College of Mechanical Engineering.

His current research interests include networked vehicular platoon control.

Mr. Zheng received the Best Student Paper Award at the 17th International IEEE Conference on Intelligent Transportation Systems in 2014, and the best paper award at the 14th Intelligent Transportation Systems Asia-Pacific Forum in 2015. He was a recipient of the National Scholarship and Outstanding Graduate in Tsinghua University.

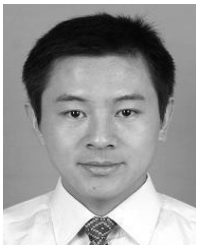

Shengbo Eben Li (M'13) received the M.S. and Ph.D. degrees from Tsinghua University, Beijing, China, in 2006 and 2009, respectively.

He was with the University of Michigan, Ann Arbor, MI, USA, from 2010 to 2012, as a Post-Doctoral Researcher. He is currently an Associate Professor with the Department of Automotive Engineering, Tsinghua University, and a Visiting Researcher with the University of California at Berkeley, Berkeley, CA, USA. He has authored or co-authored over 80 peer-reviewed journal/conference papers, and holds over ten patents. His current research interests include multiagent control and estimation, optimal control, autonomous vehicle control, driver assistance systems, and battery control.

Dr. Li was a recipient of the Award for Science and Technology from the China ITS Association in 2012, the Award for Technological Invention from the Ministry of Education in 2012, the National Award for Technological Invention in China in 2013, the Honored Funding for Beijing Excellent Youth Researcher in 2013, and several best paper awards in academia.

Keqiang Li received the B.Tech. degree from Tsinghua University, Beijing, China, in 1985, and the M.S. and Ph.D. degrees from Chongqing University, Chongqing, China, in 1988 and 1995, respectively.

He is currently a Professor of Automotive Engineering with Tsinghua University. He has authored over 90 papers and holds 12 patents in China and Japan. His current research interests include vehicle dynamics and control for driver assistance systems and hybrid electrical vehicles.

Dr. Li has served as a Senior Member of the Society of Automotive Engineers of China, and on the Editorial Boards of the *International Journal of ITS Research* and the *International Journal of Vehicle Autonomous Systems*. He was a recipient of the Changjiang Scholar Program Professor, and some awards from public agencies and academic institutions of China.

Le-Yi Wang (S'85–M'89–SM'01–F'12) received the Ph.D. degree in electrical engineering from McGill University, Montréal, QC, Canada, in 1990.

He has been with Wayne State University, Detroit, MI, USA, since 1990, where he is currently a Professor with the Department of Electrical and Computer Engineering. His current research interests include complexity and information, system identification, robust control, and H-infinity optimization.

Prof. Wang is a member of the Core International Expert Group at the Academy of Mathematics and Systems Science, Chinese Academy of Sciences, Beijing, China. He was a Keynote Speaker in several international conferences. He serves on the IFAC Technical Committee on Modeling, Identification and Signal Processing. He was an Associate Editor of the IEEE TRANSACTIONS ON AUTOMATIC CONTROL and several other journals, and is currently an Editor of the *Journal of System Sciences and Complexity* and an Associate Editor of the *Journal of Control Theory and Applications*.